J Physiol 589.15 (2011) pp 3721–3730

The Journal of Physiology

O-glycosylation of the cardiac I_{Ks} complex

Kshama D. Chandrasekhar[1], Anatoli Lvov[1], Cecile Terrenoire[2], Grace Y. Gao[1], Robert S. Kass[2] and William R. Kobertz[1]

[1]*Department of Biochemistry and Molecular Pharmacology, University of Massachusetts Medical School, Worcester, MA 01605, USA*
[2]*Department of Pharmacology, Columbia University Medical Centre, New York, NY 10032, USA*

Non-technical summary Post-translational modification of cardiac ion channels is a cellular mechanism for maintaining the rhythmicity of the heartbeat. We show that an essential regulatory subunit (KCNE1) of the cardiac I_{Ks} potassium channel complex is glycosylated at threonine-7 *in vivo*. Mutations that prevent glycosylation at this amino acid result in cardiac I_{Ks} complexes that are unable to efficiently traffic to the plasma membrane. These results provide a cellular mechanism for a KCNE1 mutation (T7I) that has been associated with cardiac arrhythmias.

Abstract Post-translational modifications of the KCNQ1–KCNE1 (Kv7) K^+ channel complex are vital for regulation of the cardiac I_{Ks} current and action potential duration. Here, we show the KCNE1 regulatory subunit is *O*-glycosylated with mucin-type glycans *in vivo*. As *O*-linked glycosylation sites are not recognizable by sequence gazing, we designed a novel set of glycosylation mutants and KCNE chimeras and analysed their glycan content using deglycosylation enzymes. Our results show that KCNE1 is exclusively *O*-glycosylated at Thr-7, which is also required for *N*-glycosylation at Asn-5. For wild type KCNE1, the overlapping *N*- and *O*-glycosylation sites are innocuous for subunit biogenesis; however, mutation of Thr-7 to a non-hydroxylated residue yielded mostly unglycosylated protein and a small fraction of mono-*N*-glycosylated protein. The compounded hypoglycosylation was equally deleterious for KCNQ1–KCNE1 cell surface expression, demonstrating that KCNE1 *O*-glycosylation is a post-translational modification that is integral for the proper biogenesis and anterograde trafficking of the cardiac I_{Ks} complex. The enzymatic assays and panel of glycosylation mutants used here will be valuable for identifying the different KCNE1 glycoforms in native cells and determining the roles *N*- and *O*-glycosylation play in KCNQ1–KCNE1 function and localization in cardiomyocytes.

(Received 26 April 2011; accepted after revision 10 June 2011; first published online 13 June 2011)

Corresponding author William R. Kobertz: Department of Biochemistry and Molecular Pharmacology, University of Massachusetts Medical School, 364 Plantation Street, Worcester, MA 01605-2324, USA. Email: william.kobertz@umassmed.edu

Abbreviations E1, KCNE1; E3, KCNE3; ER, endoplasmic reticulum; Q1, KCNQ1; T tubules, transverse tubules; WT, wild type.

DOI: 10.1113/jphysiol.2011.211284

Introduction

The rhythmicity of the heartbeat is maintained by the regulated openings and closings of ion channels. In the human heart, Kv7.1 (KCNQ1, Q1) K^+ channels obligatorily co-assemble with KCNE1 (E1) type I transmembrane peptides to form membrane-embedded complexes that generate the slow outward cardiac I_{Ks} current (Barhanin *et al.* 1996; Sanguinetti *et al.* 1996). Q1/E1 complexes are localized to the transverse tubules (T tubules) and the outer sarcolemma in rat ventricular myocytes where they are well-positioned to control the duration of the cardiac action potential (Rasmussen *et al.* 2004). Intracellular regulation of the Q1/E1 complex can shorten or lengthen the cardiac action potential duration, enabling ventricular repolarization to be in rhythm with changes in heart rate and contractility (Marx *et al.* 2002; Jespersen *et al.* 2007). Accordingly, mutations in either the Q1 or E1 subunit that result in unregulated, dysfunctional, misfolded or trafficking defective complexes give rise to cardiac arrhythmias and congenital deafness since the Q1/E1 complex is the sole entryway for potassium into the endolymph (Splawski *et al.* 1997*a*,*b*; Bianchi *et al.* 1999; Franqueza *et al.* 1999; Chouabe *et al.* 2000; Chen *et al.* 2003; Krumerman *et al.* 2004; Shamgar *et al.* 2006; Lundby *et al.* 2007).

Several post-translational modifications have been implicated in regulation and trafficking of the Q1/E1 complex. For Q1, cyclic AMP-dependent protein kinase (PKA) phosphorylation at residue S27 enhances Q1/E1 currents, which shortens the cardiac action potential duration in response to β-adrenergic receptor activation (Marx *et al.* 2002). Conversely, ubiquitination of Q1 via Nedd4-2 reduces both Q1/E1 current and steady-state levels of Q1 protein, providing a mechanism to down-regulate channel activity in cardiomyocytes and renal epithelial cells (Jespersen *et al.* 2007). In contrast to Q1, E1 post-translational modifications have not been as forthcoming. Pharmacological studies utilizing endogenous *Xenopus laevis* Q1 indicate that E1 may be phosphorylated (Busch *et al.* 1992; Zhang *et al.* 1994), but the presence, absence or removal of a phosphate group on E1 protein has not been directly shown. In addition, E1 does possess two asparagine (*N*)-glycosylation consensus sites (NXT/S) (Fig. 1*A*) and a mutation within the N5 consensus site (T7I) has been linked to Long QT and Jervell and Lange–Nielsen syndromes (Schulze-Bahr *et al.* 1997). However, the initial attachment of *N*-glycans in the ER is a *co-translational* event, though we have recently discovered that E1 acquires some of its initial *N*-glycans shortly after protein synthesis (Bas *et al.* 2011).

Here we show that E1 is *O*-glycosylated in both cell lines and cardiomyocytes. Since *O*-glycosylation does not have a recognizable consensus sequence, we utilized a panel of E1–E3 chimeras and E1 point mutants in deglycosylation assays to identify threonine-7 (T7) as the sole attachment site of mucin-type, *O*-linked glycans on E1. Simple replacement of T7 with a non-hydroxylated residue also eliminates the *N*-glycosylation consensus site at N5, which had an unexpected deleterious effect on overall glycosylation, affording mostly unglycosylated E1 subunits and a small population of monoglycosylated protein. To ameliorate this compounded hypoglycosylation and disentangle the contributions of *N*- and *O*-glycosylation on Q1/E1 anterograde trafficking and function, we developed a novel set of E1 glycosylation mutations that had different *O*- and *N*-glycan content adjacent to the E1 N-terminus. Examination of these mutants revealed that Q1/E1 complexes that lack N-terminal glycans (*N*- and *O*-) adjacent to the E1 N-terminus were functionally similar to wild type (WT), but had significantly reduced cell surface expression. Thus, mutations that directly destroy the E1 *O*-glycosylation site have a catastrophic affect on Q1/E1 biogenesis and anterograde trafficking, yielding unglycosylated and mono-*N*-glycosylated complexes that are trafficking defective and compromised, respectively.

Methods

Ethical approval

Transgenic mice expressing hKCNE1–hKCNQ1 fusion protein in the heart have been previously described (Marx *et al.* 2002). Mice were anaesthetized by intraperitoneal injection of ketamine (100 mg kg^{-1}) and xylazine (10 mg kg^{-1}) and hearts were removed following protocols approved by the Institutional Animal Care and Use Committee at Columbia University.

Plasmids and cDNAs

Human Q1 and E1 were subcloned into pcDNA3.1(–) (Invitrogen). All E1 constructs contained a C-terminal HA (YPYDVPDYA) epitope tag attached to the C-terminus of E1 via an SGSG linker, which has been previously show to yield glycosylated Q1/E1 complexes that function similar to wild type (Chandrasekhar *et al.* 2006). Chimeras of E1 and E3 were generated by cassette mutagenesis. Point mutations were introduced into E1 using QuikChange site-directed mutagenesis (Stratagene). All mutants were confirmed by sequencing the entire cDNA.

Cell culture and transfections

Chinese hamster ovary-K1 (CHO) cells were cultured in F-12K nutrient mixture (Invitrogen), supplemented with 10% fetal bovine serum (Hyclone) and 100 units ml^{-1} penicillin–streptomycin (Invitrogen). Cells were plated at 60–75% confluency in 35 mm dishes. After 24 h, the cells were transiently transfected at room temperature

(RT) with 8 μl Lipofectamine (Invitrogen) per millilitre of Opti-MEM (Gibco-Invitrogen) and returned to fresh culture media after 6 h. DNA ratios (in μg): E1/empty pcDNA 3.1 plasmid: 1.5/0.75; Q1/E1 (WT and mutants): 0.75/1.5. Cells were lysed 48 h post-transfection.

Mouse heart homogenates

Mice hearts were homogenized in 1 ml of PBS with complete protease inhibitor mixture (Roche Diagnostics, Indianapolis, IN, USA) at 4°C with a Tissuemiser homogenizer (Fisher Scientific, Pittsburgh, PA, USA). Homogenates were then centrifuged (15,000 *g*) for 25 min and supernatants were collected and used for biochemical experiments.

Cell lysis and Western blot analysis

Cells were washed in ice-cold PBS (3 × 2 ml) and lysed at 4°C in RIPKA lysis buffer (10 mM Tris·HCl, pH 7.4, 140 mM NaCl, 10 mM KCl, 1 mM EDTA, 1% Triton X-100, 0.1% SDS, 1% sodium deoxycholate), supplemented with protease inhibitors, 1 mM phenylmethylsulfonyl fluoride, and 1 μg ml^{-1} each of leupeptin, pepstatin and aprotinin. Cells were lysed in 250 μl of RIPKA buffer and the debris was pelleted in a microcentrifuge (16,100 *g* for 10 min at RT). The supernatants were diluted with SDS–PAGE loading buffer containing 100 mM dithiothreitol, separated on a 15% SDS polyacrylamide gel, and transferred to nitrocellulose (0.2 μm; Schleicher & Schuell). The membranes were blocked in blocking buffer (5% non-fat dried milk in Tris-buffered saline containing 0.2% Tween-20 (TBS-T)) for 30 min at RT and then incubated with rat anti-HA (Roche Applied Science) (1:750) in blocking buffer overnight at 4°C. For mouse heart homogenates, blots were incubated with rabbit anti-Q1 (Sigma) (1:1000) in blocking buffer for 2 h at RT. The membranes were washed in TBS-T (4 × 5 min) and incubated with goat anti-rat horseradish peroxidase-conjugated antibody (Santa Cruz Biotechnology, Inc.) (1:2000) or goat anti-rabbit horseradish peroxidase-conjugated antibody (Cell Signalling Technology) (1:3000) in blocking buffer for 30 min at RT. The membranes were subsequently washed with TBS-T (4 × 5 min). Horseradish peroxidase-bound proteins were detected by chemiluminescence using SuperSignal West Dura Extended Duration Substrate (Pierce) and a Fujifilm LAS-3000 CCD camera.

Enzymatic deglycosylation analysis

CHO cell lysates (20 μg, 30 μl) were digested with Endo H_f (3000 U, 3 μl), PNGase F (1500 U, 3 μl) (New England BioLabs, Inc.), or an enzyme cocktail containing PNGase F–neuraminidase–*O*-glycosidase (1500 U, 3 μl–150 U, 3 μl–0.5 mU, 1 μl) for 1 h at 37°C (neuraminidase and *O*-glycosidase: Roche). The RIPKA-solubilized samples were then raised to 100 mM dithiothreitol and 3.5% SDS to swamp out non-ionic detergent (Triton X-100) before resolving by SDS–PAGE (15% gel) and analysed by Western blot. Mouse heart homogenates (20 μl) were digested with PNGase F (7 μl)

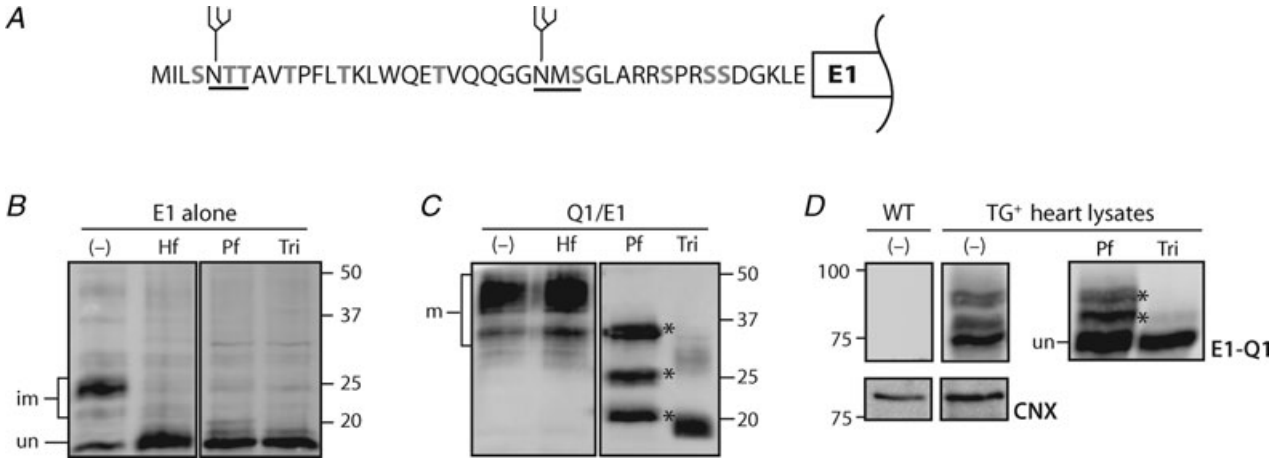

Figure 1. KCNE1 is *O*-glycosylated *in vivo*
A, N-terminal sequence of E1 depicting *N*-glycosylation sites (underlined) with core sugar structures attached to the asparagines residues. Potential *O*-linked glycosylation residues are in grey. Immunoblots from enzymatic deglycosylation of E1 subunits: *B*, E1 expressed alone in CHO cells; *C*, E1 co-expressed with Q1 channels in CHO cells; *D*, heart homogenates from a transgenic mouse (TG$^+$) expressing a E1–Q1 concatenated construct. Samples were left untreated (–), digested with Endo H (Hf), PNGase F (Pf) or an enzyme cocktail containing PNGase F, neuraminidase and *O*-glycosidase (Tri) and separated by SDS-PAGE (15%). Mature (m), immature (im) and unglycosylated (un) E1 subunits are indicated as determined by enzymatic digestion. Asterisks indicate the different *O*-glycoforms that were cleaved with *O*-glycosidase. CNX (calnexin) loading control for the WT and TG$^+$ lysates.

or an enzyme cocktail containing PNGase F–neuraminidase–*O*-glycosidase (7 μl–7 μl–7 μl) for 1 h at 37°C since the enzymes are less effective on membrane integrated substrates. The PBS-homogenates were then raised to 100 mM dithiothreitol and 5% SDS before resolving by SDS–PAGE (6% gel) and analysed by Western blot.

Cell surface biotinylation

Cells were rinsed with ice-cold PBS^{2+} buffer (4 × 2 ml; PBS containing 1 mM $MgCl_2$, 0.1 mM $CaCl_2$) at 4°C to arrest cellular trafficking. The cell surface proteins were labelled with 1 mg ml^{-1} sulfo-NHS-SS-biotin (Pierce) in PBS^{2+} buffer twice for 15 min at 4°C. To quench the excess biotinylation reagent, the cells were washed (3 × 2 ml) with quench solution (PBS^{2+} containing 100 mM glycine) and then incubated with quench solution twice for 15 min at 4°C. The cells were lysed in RIPKA buffer for 30 min at 4°C. Cell debris was removed by centrifugation (16,100 *g* for 10 min at 4°C). Total protein in each sample was quantitated by bicinchonimic acid (BCA) analysis. Of these samples, 150 μg of total protein was separated by affinity chromatography on 25 μl of Immunopure immobilized streptavidin beads (Pierce) overnight at 4°C, whereas 30 μg was saved as an input control to determine the percentage of biotinylated proteins. The beads were washed (3 × 500 μl) in 0.1% SDS wash buffer (10 mM Tris·HCl, pH 7.4, 150 mM NaCl, 1 mM EDTA, 0.1% SDS). Biotinylated proteins were eluted from the beads using 2 × SDS–PAGE loading buffer with 200 mM dithiothreitol for 15 min at 55°C. The inputs and eluted proteins were both divided and resolved separately by SDS–PAGE (15% gel). One Western blot was probed for E1 whereas the other blot was probed for calnexin – an ER resident protein used as a control to determine the percentage of cell rupture that occurred during the labelling process. Calnexin blots were incubated with rabbit anti-calnexin (Chemicon) (1:4000) and donkey anti-rabbit horseradish peroxidase-conjugated antibody (Promega) (1:8000) as described in the Western blot analysis methods. The images of non-saturated bands were captured on a Fujifilm LAS-3000 CCD camera, and total band intensities on the blots were quantitated using MultiGauge V2.1 software (FujiFilm) to account for all glycosylated forms of E1. Background cell lysis was quantitated as a ratio of biotinylated calnexin protein to total input calnexin for each sample. The percentage of E1 protein on the cell surface was calculated from the ratio of avidin-bound protein to total input protein after background lysis subtraction.

Perforated patch whole-cell recordings

CHO cells were transiently transfected (in micrograms per dish) with 0.75 Q1, 1.5 E1 (WT or mutant) and 0.25 pEGFP-C3. Cells were used 24–48 h post-transfection. Currents were recorded in the perforated patch configuration as described previously (Lvov *et al.* 2010). Briefly, on the day of the experiment, cells were seeded onto glass coverslips and placed in a recording chamber filled with extracellular solution containing (in mM): 160 NaCl, 2.5 KCl, 2 $CaCl_2$, 1 $MgCl_2$, 8 glucose and 10 Hepes (pH 7.5 with NaOH). The glass electrode (pipette resistance: 2.5–3.5 MΩ) filled with electrode solution containing (in mM): 126 KCl, 1 $MgSO_2$, 0.5 $CaCl_2$, 5 EGTA, 4 K_2-ATP, 0.4 GTP, 25 Hepes (pH 7.5 with CsOH) and 60 μg ml^{-1} Amphotericin B (Sigma; prepared in DMSO) was attached to the transfected (eGFP-expressing) cell. Electrical access to the inside of the cell was monitored using a 3 s depolarizing test pulse from the holding potential of −80 mV to +20 mV taken every 15 s. Once the access resistance was dropped to a level suitable to record the membrane potential (<10 MΩ), a family of currents was measured from −100 to +60 mV in 10 mV increments. All measurements were performed at room temperature (24 ± 2°C).

Data analysis

The amplitude of tail currents was measured 5 ms after repolarization to –30 mV and normalized such that the maximal current was equal to 1. Normalized tail currents were plotted *versus* the depolarized potential to produce activation curves for WT and mutant Q1/E1 channel complexes. Activation curves were fitted to a Boltzmann function, $I/I_{max} = A2 + (A1 - A2) / (1 + e^{(V - V_{1/2})*(-zF/RT)})$, where I/I_{max} is the normalized tail current amplitude, $V_{1/2}$ is the mid-point of activation, z is the maximum slope or apparent gating valence, F is Faraday's constant, R is the gas constant and T is temperature in Kelvin. The deactivation time constant ($\tau_{deactivation}$) for WT Q1/E1 and the glycosylation mutants were measured by fitting the tail currents at –30 mV to a single exponential.

Results

We have previously shown that the *N*-glycosylation state of E1 subunits can be used to follow their migration through the biosynthetic pathway (Chandrasekhar *et al.* 2006); these studies suggested that E1 acquired a post-translational modification that was not removable with *N*-glycanases. Figure 1 exemplifies how this traditional enzymatic approach works with a C-terminally, HA-tagged E1 protein expressed in CHO cells. E1 protein that is susceptible to Endo H (Hf) treatment is immaturely *N*-glycosylated protein, which is predominately found in the ER as well as the *cis* Golgi whereas E1 protein that is Endo H resistant and PNGase F sensitive corresponds

to maturely *N*-glycosylated protein that has trafficked beyond the *cis* Golgi (Chandrasekhar *et al.* 2006). The enzymatic profile in Fig. 1*B* demonstrates that when E1 is expressed alone it is immaturely *N*-glycosylated and localized to the early compartments of the biosynthetic pathway (ER and *cis* Golgi) since the ∼24 kDa band was susceptible to both Endo H and PNGase F. In contrast, transient expression of Q1/E1 in CHO cells (Fig. 1*C*) afforded E1 protein with three distinctively different biochemical behaviours that suggested the presence of a post-translational modification: (1) The mobility of E1 in denaturing polyacrylamide gels was substantially retarded, migrating as a strong, but diffuse band between 40–50 kDa and a fainter set of bands starting at 35 kDa. (2) The protein was completely resistant to Endo H treatment, which indicates that the two *N*-glycans on the E1 subunits had matured in the Golgi apparatus. (3) PNGase F digestion was incomplete, producing three digestion products (indicated by asterisks) that migrated slower than unglycosylated E1.

Since the putative protein modification was only on E1 subunits that had mature *N*-glycosylation, we reasoned that the post-translational modification(s) was occurring in the Golgi. This conjecture prompted us to determine whether E1 was modified with mucin-type (*O*-GalNAc) glycans (Hanisch, 2001) when co-expressed with Q1. To do this, we used a cocktail of deglycosylation enzymes: neuraminidase to remove the sialic acid sugars from *N*- and *O*-glycans, which enables efficient cleavage of *O*-glycans by *O*-glycosidase; and *O*-glycosidase and PNGase F to remove the *O*- and *N*-glycans, respectively. Lysates from CHO cells co-expressing Q1 and E1 subunits were digested with the enzyme cocktail (Tri) that resulted in complete loss of the residual bands with a corresponding accumulation of unglycosylated E1 protein at 18 kDa (Fig. 1*C*), showing that mature E1 subunits are *O*-glycosylated. *O*-glycosylation of E1 is not a CHO-cell-specific modification since a similar set of PNGase F-resistant bands was observed for E1 protein expressed in different mammalian cell lines (Chandrasekhar *et al.* 2006). In contrast, immaturely *N*-glycosylated E1 subunits were not *O*-glycosylated (Fig. 1*B*, compare Pf and Tri), which is also consistent with *O*-glycosylation since mammalian mucin-type transferase enzymes are specifically localized to the Golgi (Hanisch, 2001).

Although the presence of *O*-glycans explains the differences in electrophoretic mobility and enzymatic susceptibility of E1 proteins expressed in mammalian cell lines, post-translational modifications in the Golgi can be cell type specific (Jacobs & Callewaert, 2009). Therefore, we determined whether E1 subunits were *O*-glycosylated in cardiomyocytes. Part of the elusiveness of identifying this modification in native cells has been that antibodies generated against E1 protein efficiently recognize the ∼15–25 kDa bands, which correspond to the immaturely and unglycosylated forms of E1 that have yet to reach the Golgi (Chandrasekhar *et al.* 2006). To circumvent this antigenicity problem, we exploited a Q1/E1 transgenic mouse model since the cardiac I_{Ks} current is not detectable in WT mice (Marx *et al.* 2002). These TG^+ mice stably express a concatenated human E1–Q1 fusion protein that has the C-terminus of E1 linked to the N-terminus of Q1 in the cytoplasm (Wang *et al.* 1998). Human I_{Ks} currents recorded from TG^+ cardiomyocytes are functionally indistinguishable from unconcatenated human cardiac I_{Ks}; moreover, the concatenated Q1/E1 complex in murine myocytes interacts with the same post-translational machinery identified in human heart (Marx *et al.* 2002; Dilly *et al.* 2004; Sampson *et al.* 2008). For this study, the E1–Q1 fusion protein enabled us to detect the different glycosylation states of the E1 N-terminus using anti-Q1 antibodies. Figure 1*D* shows Western blots from heart homogenates from WT and TG^+ mice. Using a Q1 antibody, several bands from ∼75 to 100 kD were only observed in heart homogenates from the TG^+ mice (calnexin (CNX) loading control shown below). Enzymatic deglycosylation with PNGase F increased the intensity of the lower bands, but residual bands (asterisks) could not be completely digested. However, addition of neuraminidase and *O*-glycosidase to the enzyme cocktail (Tri) resulted in complete digestion, which showed that the cardiac I_{Ks} complex is *O*-glycosylated *in vivo*.

Having confirmed that the cardiac I_{Ks} complex is *O*-glycosylated, we next determined which E1 residue(s) acquired *O*-glycans. The E1 N-terminus contains numerous threonine and serine residues that could serve as *O*-glycan attachment sites (Fig. 1*A*, grey residues). In addition, mucin-type *O*-glycosylation tends to cluster on proteins (Hanisch, 2001), making it challenging to identify the individual attachment sites. To narrow down the regions of the E1 N-terminus where *O*-glycan attachment could occur, we made N-terminal KCNE chimeras (Fig. 2*A*) between E1 and KCNE3 (E3) – a KCNE that is only *N*-glycosylated and provides a suitable *O*-glycan-deficient background (Gage & Kobertz, 2004). The two chimeras were co-expressed with Q1 in CHO cells and the different glycoforms were separated by SDS–PAGE (Fig. 2*B*). The increased gel mobility of the untreated Chi2 chimera (compared to WT and Chi1 chimera) immediately hinted that the *O*-glycosylation sites were located near the E1 N-terminus. Endo H treatment identified the chimeric proteins that were modified in the Golgi; enzymatic treatment with PNGase F and the enzyme cocktail (Tri) confirmed that the *O*-glycosylation site(s) were in the top half of the E1 N-terminus.

In the absence of defined protein consensus sites for mucin-type *O*-glycosylation, we analysed the E1 N-terminus (resides 1–25) using the NetOGlyc3.1 algorithm (Hamby & Hirst, 2008), which returned two

potential *O*-glycosylation sites at threonines 6 and 7 (T6 and T7). Mutation of T6 to alanine showed the same gel mobility and enzymatic susceptibility as WT, indicating that the T6A mutant was still *O*-glycosylated (Fig. 2*C*). To test for *O*-glycosylation at T7, we initially tested the T7A mutation even though it would destroy the N-terminal *N*-glycosylation site at N5. Surprisingly, the biogenesis of the T7A mutant was severely compromised, yielding mostly unglycosylated protein and a small amount of mono-*N*-glycosylated protein (Fig. 2*C*), which we have recently shown is due to the kinetics of *N*-glycan attachment in the ER (Bas *et al.* 2011). Thwarted by the compounded hypoglycosylation of the T7A mutant, we designed a mutant (T6F) *in silico* using NetOglyc3.1 that would acquire an *N*-glycan at N5, but was predicted not to be *O*-glycosylated at T7. Co-expression of T6F with Q1 resulted in a broad range of bands from 20 to 50 kDa (Fig. 2*C*). Most of the bands were unaffected by Endo Hf treatment, indicating that the T6F mutant was modified in the Golgi. Treatment with PNGase F collapsed all of the bands to unglycosylated, which demonstrated that T6F mutant prevented *O*-glycosylation. Although the T6F mutant eliminated *O*-glycosylation of the E1 N-terminus, this result could not rule out *O*-glycosylation at both T6 and T7. To rule out *O*-glycosylation at T6, we engineered a secondary mutation (S28T) into the T7A mutant, which promotes efficient *N*-glycosylation at N26 (Bas *et al.* 2011). In contrast to T7A, co-expression of the T7A(S28T) mutant with Q1 resulted in predominately mature *N*-glycosylated E1 protein that lacked *O*-glycosylation (Fig. 2*C*), identifying T7 as the sole site of E1 *O*-glycosylation.

We next determined whether the *N*- and *O*-glycan content adjacent to the E1 N-terminus altered the cell surface expression and biophysical properties of the Q1/E1 complex. Since the T7A mutant obliterated all glycosylation and cell surface expression (data not shown), we exploited the S28T mutation and generated a panel of E1 mutants that lacked either the N-terminal *N*-linked or *O*-linked site, or both sites (Fig. 3*A*). To directly measure the cell surface population of the differently glycosylated E1 mutants, we used cell surface biotinylation in CHO cells since the anterograde trafficking of E1 is dependent on co-assembly with Q1 in this cell line (Chandrasekhar *et al.* 2006). Cells expressing WT or glycosylation mutant Q1/E1 complexes were labelled with a membrane-impermeant, amine-reactive biotin reagent at 4°C to prevent membrane recycling and minimize labelling of intracellular proteins. The biotinylated proteins were isolated with streptavidin beads and analysed by Western blot (Fig. 3*B*). To verify

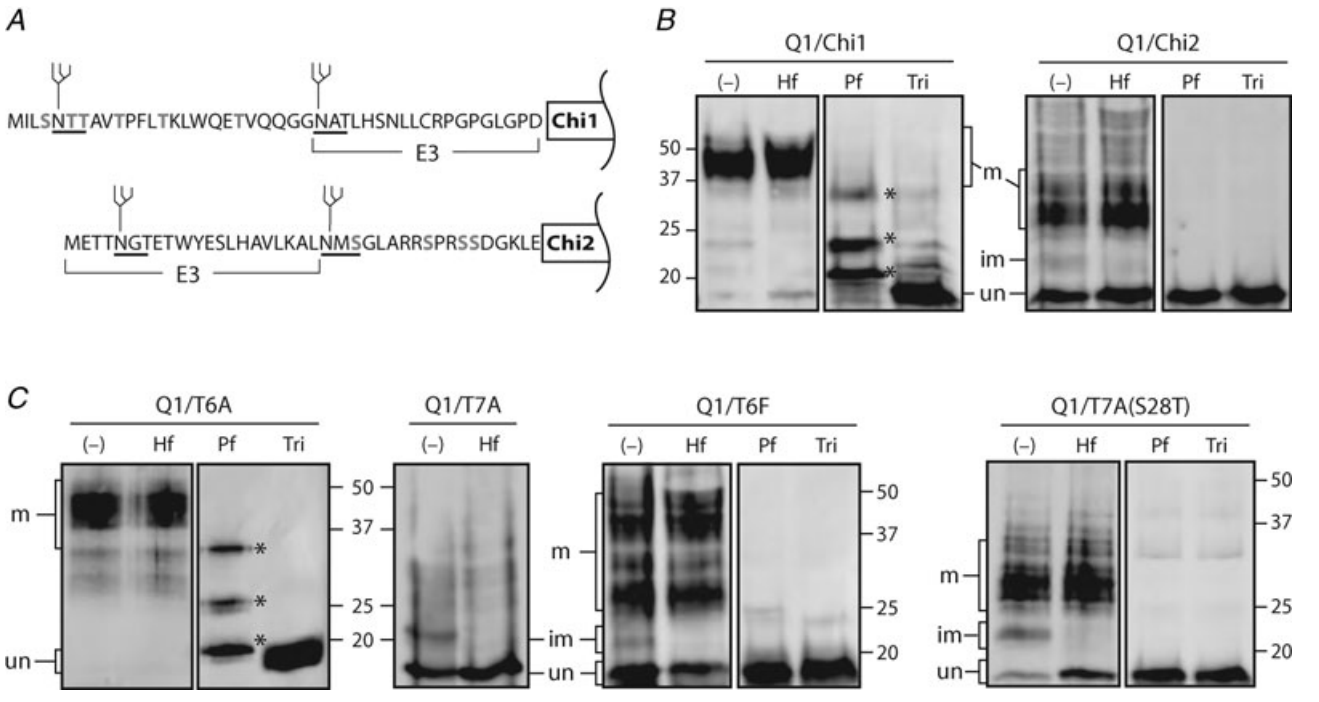

Figure 2. KCNE1 subunits are *O*-glycosylated at threonine-7
A, N-terminal amino acid sequences of the E1/E3 protein chimeras (Chi1, Chi2). *N*-glycosylation sites are underlined and the potential *O*-linked sites are shown in grey. *B*, immunoblots of enzymatic deglycosylation of E1/E3 chimeras, and *C*, E1 glycosylation mutants co-expressed with Q1 in CHO cells. Samples were left untreated (–), digested with Endo H (Hf), PNGase F (Pf) or an enzyme cocktail of PNGase F, neuraminidase and *O*-glycosidase (Tri) and separated by SDS-PAGE (15%). Mature (m), immature (im) and unglycosylated (un) samples are indicated as determined by enzymatic digestion. Asterisks denote *O*-glycosylated E1 protein.

that the cells remained intact during biotinylation, we monitored the labelling of an ER-resident protein (calnexin: CNX) and subtracted out the background intracellular labelling to calculate the cell surface expression of the E1 glycosylation mutants, which were normalized to WT (Fig. 3*C*). Q1/E1 complexes with either an *N*-glycan (T6F) or *O*-glycan (N5Q/S28T) adjacent to the E1 N-terminus had similar cell surface expression as WT. However, E1 subunits lacking both N-terminal glycans (T7A/S28T) had a trafficking defect, resulting in ∼50% reduction of Q1/E1 complexes at the cell surface.

To determine whether the N-terminal glycans contributed to the unique voltage-gating of the Q1/E1 channel complex, we examined the glycosylation mutants in CHO cells using the perforated patch configuration. Families of currents were generated for WT and glycosylation mutant Q1/E1 complexes (Fig. 4). Q1/E1 complexes that lacked *O*-, *N*- or both glycans adjacent to the E1 N-terminus had voltage dependence and activation gating at the $V_{1/2}$ that was not significantly different than WT (Fig. 4). Q1/E1 deactivation (Table 1) was inversely influenced by E1 N-terminal glycosylation: prevention of *O*-glycosylation (T6F) accelerated closing; prevention of *N*-glycosylation (N5Q/S28T) slowed closing. Barring the modest deactivation effects, these results show that Q1/E1 complexes that fail to acquire E1 N-terminal glycans (*N*- and *O*-) function similar to WT, but have significantly reduced cell surface expression.

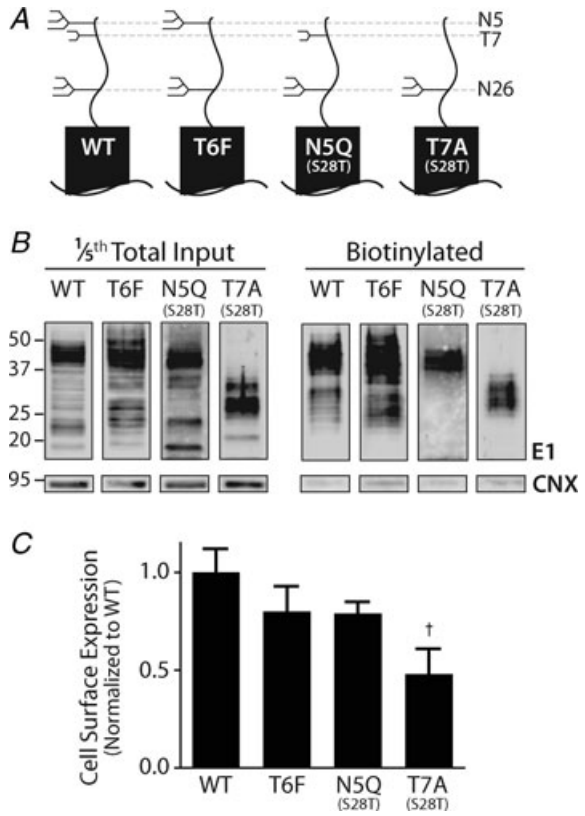

Figure 3. KCNE1 subunits lacking *N*- and *O*-glycosylation adjacent to the N-terminus have reduced cell surface expression
A, cartoon depiction of the E1 glycosylation mutants. *B*, representative immunoblots, and *C*, cell surface quantification of WT and E1 glycosylation mutants co-expressed with Q1 channels in CHO cells. Lanes denoted as '1/5th total input' are a portion of the sample lysate that was set aside to quantitate the total amount of biotinylated proteins. Biotinylated lanes represent the cell surface biotinylated proteins that were isolated with streptavidin and separated by SDS–PAGE. Calnexin (CNX) immunoblot approximates the amount of cell lysis that occurs during the labelling process. The cell surface expression of the glycosylation mutants was calculated as described in the Methods and normalized to WT expression. Error bars indicate standard error measurement (S.E.M.) from three immunoblots. †$P < 0.05$ (1-way ANOVA with Tukey *post hoc* analysis).

Discussion

We have shown the cardiac I_{Ks} complex is *O*-glycosylated *in vivo* and have identified T7 as the lone attachment site for mucin-type *O*-glycans on E1. Similar to *N*-glycosylation, *O*-glycosylation of E1 is heterogeneous. Enzymatic removal of the *N*-linked glycans (Fig. 1, Pf lanes) demonstrated that there are at least two predominant E1 *O*-glycoforms in heart and three in CHO cells. Post-translational modification of E1 with *O*-glycans also explains the vastly different mobilities of E1 protein on Western blots: 15–25 kD bands are the unglycosylated and immaturely *N*-glycosylated E1 protein found predominately in the ER; 37–50 kD bands are E1 proteins with mature *N*-glycans and *O*-glycans; 25–37 kD bands correspond to E1 protein with either less-extensive overall glycosylation or with unmodified glycosylation sites. Although the accrual of glycans on E1 in the Golgi correlated with their gel shift mobilities, this relationship is neither linear nor straightforward. E1 subunits with two or three glycans had similar electrophoretic mobilities whereas monoglycosylated E1 subunits migrated faster on SDS–PAGE (Fig. 3*B*). The unpredictable gel mobilities of the differently glycosylated E1 proteins underscores the importance of a quick enzymatic digest to identify both the composition and maturity of glycans on this family of small type I transmembrane peptides.

Previous *O*-glycosylation studies of K^+ channel complexes have focused on the negatively charged, terminal sialic acids (Ufret-Vincenty *et al.* 2001; Schwetz *et al.* 2011), presumably due to the significant challenge in identifying *O*-linked glycosylation sites on polytopic membrane proteins. As a single-pass transmembrane peptide, locating the E1 *O*-glycosylation site (T7) was easier, though complicated by the fact that this threonine is also part of the N-terminal *N*-glycosylation consensus sequence (NTT). For wild type E1 subunits, this overlap is a non-issue – an unmodified hydroxylated residue

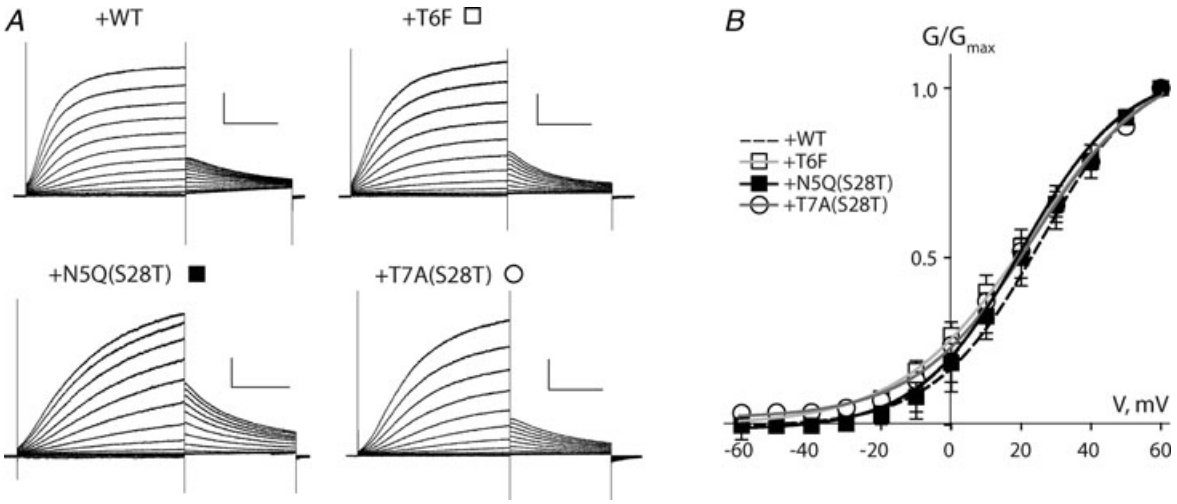

Figure 4. Wild type and KCNE1 glycosylation mutants have similar electrophysiological properties
A, representative families of I_{Ks} current traces recorded from CHO cells in the perforated patch configuration. Cells were held at −80 mV, subjected to 3 s command potentials ranging from −100 mV to +60 mV in 10 mV increments followed by a 1 s tail pulse at −30 mV. Scale bars are 0.5 nA and 0.5 s. *B*, voltage activation curves were obtained by plotting normalized tail currents *versus* the pre-pulse potential. Values for the midpoint of activation ($V_{1/2}$) were obtained by fitting with the Boltzmann equation (lines) as described in the Methods.

in the consensus sequence is only needed for the initial attachment of an *N*-glycan in the ER (Helenius & Aebi, 2004), but is not required for the subsequent trimming or additions of *N*-glycans in the Golgi where *O*-glycosylation occurs (Hanisch, 2001). However, mutations in the overlapping glycosylation consensus sites had multifarious consequences for E1 biogenesis and trafficking (Figs 2 and 3). Mutations that selectively prevented glycosylation at either site adjacent to the E1 N-terminus (N5 or T7) had no measurable effect on assembly with Q1 and trafficking of the Q1/E1 complex. Prevention of all glycosylation adjacent to the E1 N-terminus had an intermediate effect on Q1/E1 trafficking, reducing cell surface expression by 50% when compared to WT. The most deleterious mutation was T7A, which destroyed both N-terminal glycosylation sites and indirectly inhibited *N*-glycan attachment to N26, yielding unglycosylated E1 subunits that do not reach the plasma membrane. Thus, the overlapping glycosylation sites in E1 enable a single point mutation to obliterate E1 glycosylation and cell surface expression, which we have recently shown to be the case for the Long QT mutant, T7I (Bas *et al.* 2011).

We have long suspected that E1 acquired a post-translational modification when co-expressed with Q1, but we were initially hesitant to confirm our suspicions in native cells because in our hands α-E1 (commercial and in-house) antibodies only recognize the immaturely and unglycosylated forms of E1. For this reason, we (and presumably others) have used exogenously expressed epitope-tagged versions of E1. Heart homogenates from the TG^{+} mouse ameliorated the E1 antigenicity problem, allowing us to use an α-Q1 antibody to visualize the maturely *N*-glycosylated

Table 1. Electrophysiological properties of KCNE1 mutants[a]

Construct	Glycosylation	$V_{1/2}$ (mV)	z	$\tau_{deactivation}$ (ms)	t_o (ms)	pA pF^{-1}
E1	N5, T7, N26	24.8 ± 2.5	1.74 ± 0.09	794 ± 47	1338 ± 170	66.6 ± 19.5
T6F	N5, N26	22.0 ± 4.2	1.42 ± 0.06	603 ± 15	920 ± 70	67.5 ± 19.9
N5Q(S28T)	T7, N26	20.1 ± 2.7	1.07 ± 0.03	1080 ± 50†	1205 ± 90	85.7 ± 17.6
T7A(S28T)	N26	24.3 ± 2.4	1.53 ± 0.12	1210 ± 60†	1454 ± 160	62.6 ± 13.8

[a]Data are from individual activation curves and deactivation time constants obtained from three to eight CHO cells. Activation curves were fitted to a Boltzmann function as described in the Methods. $V_{1/2}$ is the voltage of half-maximal activation and z is the apparent gating valence. Time constants of deactivation were fitted to a single exponential as described in Methods. Non-exponential, activation kinetics was quantified by the time required for half-opening, t_0, at 20 mV, which is near $V_{1/2}$ for all constructs. Peak current density is presented as pA pF^{-1}. Values are mean ± SEM. †$P < 0.05$ (1-way ANOVA with Tukey *post hoc* analysis) compared to WT and T6F.

and *O*-glycosylated E1 N-terminus of the E1–Q1 fusion protein. It is remotely possible that Q1 (instead of E1) is *O*-glycosylated in this transgenic mouse; however, Q1 has no predicted *O*-linked sites and is not glycosylated in cells where E1 is fully decorated with both *O*- and *N*-glycans. Barring this unlikely scenario, the presence of an *O*-glycosylated human I_{Ks} complex in TG^+ mouse cardiomyocytes strongly argues that E1 subunits are *O*-glycosylated in human heart. Since detecting these physiologically relevant E1 glycoforms in native tissues still remains a challenge, the triumvirate of enzymes used here provides a makeshift solution to generate unglycosylated E1 protein that is detectable with currently available α-E1 antibodies. While not perfect, this enzymatic approach should allow for indirect visualization and quantification of the maturely *N*- and *O*-glycosylated E1 protein in native tissues. Moreover, complete deglycosylation may improve Q1/E1 co-immunoprecipitations from native tissues, which are notoriously inefficient and require large amounts (horse heart) of tissue (Finley *et al.* 2002).

Although both *N*- and *O*-glycosylation of E1 is hauntingly similar in cardiomyocytes and CHO cells, our results do not address whether these glycans contribute to localization of Q1/E1 complexes to the T tubules and outer sarcolemma. Similarly, the modest functional changes that we observed upon systematic glycan removal may be due to the lack of glycocalyx-filled T tubules, which greatly slow cation diffusion (Shepherd & McDonough, 1998; Swift *et al.* 2006). The panel of E1 glycosylation mutants utilized here will be useful tools for dissecting the roles *N*- and *O*-glycans play in Q1/E1 trafficking, localization and function in cardiomyocytes and other cells where E1 regulatory subunits are expressed.

References

Barhanin J, Lesage F, Guillemare E, Fink M, Lazdunski M & Romey G (1996). K_VLQT1 and IsK (minK) proteins associate to form the I_{KS} cardiac potassium current. *Nature* **384**, 78–80.

Bas T, Lvov A, Gao Y, Chandrasekhar KD, Gilmore R & Kobertz WR (2011). Post-translational N–glycosylation of type I transmembrane KCNE1 peptides: implications for membrane protein biogenesis and disease. *J Biol Chem* (in press).

Bianchi L, Shen Z, Dennis AT, Priori SG, Napolitano C, Ronchetti E *et al.* (1999). Cellular dysfunction of LQT5-minK mutants: abnormalities of I_{Ks}, I_{Kr} and trafficking in long QT syndrome. *Hum Mol Genet* **8**, 1499–1507.

Busch AE, Varnum MD, North RA & Adelman JP (1992). An amino acid mutation in a potassium channel that prevents inhibition by protein kinase C. *Science* **255**, 1705–1707.

Chandrasekhar KD, Bas T & Kobertz WR (2006). KCNE1 subunits require co-assembly with K^+ channels for efficient trafficking and cell surface expression. *J Biol Chem* **281**, 40015–40023.

Chen YH, Xu SJ, Bendahhou S, Wang XL, Wang Y, Xu WY *et al.* (2003). KCNQ1 gain-of-function mutation in familial atrial fibrillation. *Science* **299**, 251–254.

Chouabe C, Neyroud N, Richard P, Denjoy I, Hainque B, Romey G *et al.* (2000). Novel mutations in KvLQT1 that affect I_{ks} activation through interactions with Isk. *Cardiovasc Res* **45**, 971–980.

Dilly KW, Kurokawa J, Terrenoire C, Reiken S, Lederer WJ, Marks AR & Kass RS (2004). Overexpression of β2-adrenergic receptors cAMP-dependent protein kinase phosphorylates and modulates slow delayed rectifier potassium channels expressed in murine heart: evidence for receptor/channel co-localization. *J Biol Chem* **279**, 40778–40787.

Finley MR, Li Y, Hua F, Lillich J, Mitchell KE, Ganta S *et al.* (2002). Expression and coassociation of ERG1, KCNQ1, and KCNE1 potassium channel proteins in horse heart. *Am J Physiol Heart Circ Physiol* **283**, H126–H138.

Franqueza L, Lin M, Shen J, Splawski I, Keating MT & Sanguinetti MC (1999). Long QT syndrome-associated mutations in the S4–S5 linker of KvLQT1 potassium channels modify gating and interaction with minK subunits. *J Biol Chem* **274**, 21063–21070.

Gage SD & Kobertz WR (2004). KCNE3 truncation mutants reveal a bipartite modulation of KCNQ1 K^+ channels. *J Gen Physiol* **124**, 759–771.

Hamby SE & Hirst JD (2008). Prediction of glycosylation sites using random forests. *BMC Bioinformatics* **9**, 500.

Hanisch FG (2001). O–glycosylation of the mucin type. *Biol Chem* **382**, 143–149.

Helenius A & Aebi M (2004). Roles of N–linked glycans in the endoplasmic reticulum. *Annu Rev Biochem* **73**, 1019–1049.

Jacobs PP & Callewaert N (2009). N–glycosylation engineering of biopharmaceutical expression systems. *Curr Mol Med* **9**, 774–800.

Jespersen T, Membrez M, Nicolas CS, Pitard B, Staub O, Olesen SP, Baro I & Abriel H (2007). The KCNQ1 potassium channel is down-regulated by ubiquitylating enzymes of the Nedd4/Nedd4-like family. *Cardiovasc Res* **74**, 64–74.

Krumerman A, Gao X, Bian JS, Melman YF, Kagan A & McDonald TV (2004). An LQT mutant minK alters KvLQT1 trafficking. *Am J Physiol Cell Physiol* **286**, C1453–C1463.

Lundby A, Ravn LS, Svendsen JH, Olesen SP & Schmitt N (2007). KCNQ1 mutation Q147R is associated with atrial fibrillation and prolonged QT interval. *Heart Rhythm* **4**, 1532–1541.

Lvov A, Gage SD, Berrios V & Kobertz WR (2010). Identification of a protein-protein interaction between KCNE1 and the activation gate machinery of KCNQ1. *J Gen Physiol* **135**, 607–618.

Marx SO, Kurokawa J, Reiken S, Motoike H, D'Armiento J, Marks AR & Kass RS (2002). Requirement of a macromolecular signalling complex for beta adrenergic receptor modulation of the KCNQ1-KCNE1 potassium channel. *Science* **295**, 496–499.

Rasmussen HB, Moller M, Knaus HG, Jensen BS, Olesen SP & Jorgensen NK (2004). Subcellular localization of the delayed rectifier K^+ channels KCNQ1 and ERG1 in the rat heart. *Am J Physiol Heart Circ Physiol* **286**, H1300–H1309.

Sampson KJ, Terrenoire C, Cervantes DO, Kaba RA, Peters NS & Kass RS (2008). Adrenergic regulation of a key cardiac potassium channel can contribute to atrial fibrillation: evidence from an I_{Ks} transgenic mouse. *J Physiol* **586**, 627–637.

Sanguinetti MC, Curran ME, Zou A, Shen J, Spector PS, Atkinson DL & Keating MT (1996). Coassembly of K_VLQT1 and minK (IsK) proteins to form cardiac I_{Ks} potassium channel. *Nature* **384**, 80–83.

Schulze-Bahr E, Wang Q, Wedekind H, Haverkamp W, Chen Q, Sun Y *et al.* (1997). KCNE1 mutations cause Jervell and Lange-Nielsen syndrome. *Nat Genet* **17**, 267–268.

Schwetz TA, Norring SA, Ednie AR & Bennett ES (2011). Sialic acids attached to O–glycans modulate voltage-gated potassium channel gating. *J Biol Chem* **286**, 4123–4132.

Shamgar L, Ma L, Schmitt N, Haitin Y, Peretz A, Wiener R, Hirsch J, Pongs O & Attali B (2006). Calmodulin is essential for cardiac I_{KS} channel gating and assembly: impaired function in long-QT mutations. *Circ Res* **98**, 1055–1063.

Shepherd N & McDonough HB (1998). Ionic diffusion in transverse tubules of cardiac ventricular myocytes. *Am J Physiol Heart Circ Physiol* **275**, H852–H860.

Splawski I, Timothy KW, Vincent GM, Atkinson DL & Keating MT (1997*a*). Molecular basis of the long-QT syndrome associated with deafness. *N Engl J Med* **336**, 1562–1567.

Splawski I, Tristani-Firouzi M, Lehmann MH, Sanguinetti MC & Keating MT (1997*b*). Mutations in the hminK gene cause long QT syndrome and suppress I_{Ks} function. *Nat Genet* **17**, 338–340.

Swift F, Stromme TA, Amundsen B, Sejersted OM & Sjaastad I (2006). Slow diffusion of K^+ in the T tubules of rat cardiomyocytes. *J Appl Physiol* **101**, 1170–1176.

Ufret-Vincenty CA, Baro DJ & Santana LF (2001). Differential contribution of sialic acid to the function of repolarizing K^+ currents in ventricular myocytes. *Am J Physiol Cell Physiol* **281**, C464–C474.

Wang W, Xia J & Kass RS (1998). MinK-KvLQT1 fusion proteins, evidence for multiple stoichiometries of the assembled I_{sK} channel. *J Biol Chem* **273**, 34069–34074.

Zhang ZJ, Jurkiewicz NK, Folander K, Lazarides E, Salata JJ & Swanson R (1994). K^+ currents expressed from the guinea pig cardiac I_{sK} protein are enhanced by activators of protein kinase C. *Proc Natl Acad Sci U S A* **91**, 1766–1770.

Author contributions

K.D.C., A.L. and G.Y.G. contributed to data collection and analysis. K.D.C. and W.R.K. designed the experiments and wrote the manuscript. C.T. and R.S.K. provided heart homogenates from wild type and transgenic mice. All authors have approved the final version of the manuscript.

Acknowledgements

The authors declare that they have no competing financial interests. This work was supported by a grant to W.R.K. from the National Institutes of Health (DC-007669).